NJC

Accepted Manuscript

This is an *Accepted Manuscript*, which has been through the Royal Society of Chemistry peer review process and has been accepted for publication.

Accepted Manuscripts are published online shortly after acceptance, before technical editing, formatting and proof reading. Using this free service, authors can make their results available to the community, in citable form, before we publish the edited article. We will replace this *Accepted Manuscript* with the edited and formatted *Advance Article* as soon as it is available.

You can find more information about *Accepted Manuscripts* in the Information for Authors.

Please note that technical editing may introduce minor changes to the text and/or graphics, which may alter content. The journal's standard Terms & Conditions and the Ethical guidelines still apply. In no event shall the Royal Society of Chemistry be held responsible for any errors or omissions in this *Accepted Manuscript* or any consequences arising from the use of any information it contains.

ROYAL SOCIETY OF CHEMISTRY

www.rsc.org/njc

Journal Name

RSCPublishing

ARTICLE

Synthesis and Structural Characterization of Amido Heteroscorpionate Rare-Earth Metal Complexes. Hydroamination of Aminoalkenes

Cite this: DOI: 10.1039/xoxxoooooox

Received ooth January 2012,
Accepted ooth January 2012

DOI: 10.1039/xoxxoooooox

www.rsc.org/

Antonio Otero,[a]* Agustín Lara-Sánchez,[a]* José A. Castro-Osma,[a] Isabel Márquez-Segovia,[a] Carlos Alonso-Moreno,[b] Juan Fernández-Baeza,[a] Luis F. Sánchez-Barba[a] and Ana M. Rodríguez[c].

The synthesis, characterization and fluxional behaviour of novel heteroscorpionate rare-earth (including the group 3 metals scandium and yttrium) complexes are reported. The reaction of acetamide and thioacetamide heteroscorpionate protio ligands pbptamH, tbptamH, pbpamH and (*S*)-mbpamH with 1 *equiv* of the tris(silylamide) precursors $[M\{N(SiHMe_2)_2\}_3(thf)_n]$ (n = 1, M = Sc; n = 2, M = Y, Lu) proceed to give good yields of the neutral heteroscorpionate disilylamide complexes $[M\{N(SiHMe_2)_2\}_2(\kappa^3\text{-pbptam})(thf)_n]$ (M = Sc, n = 0, **1**; M = Y, n = 1, **2**; M = Lu, n = 1, **3**), $[M\{N(SiHMe_2)_2\}_2(\kappa^3\text{-tbptam})(thf)_n]$ (M = Sc, n = 0, **4**; M = Y, n = 1, **5**; M = Lu, n = 1, **6**), $[M\{N(SiHMe_2)_2\}_2(\kappa^3\text{-pbpam})(thf)_n]$ (M = Sc, n = 0, **7**; M = Y, n = 1, **8**; M = Lu, n = 1, **9**) and $[M\{N(SiHMe_2)_2\}_2\{\kappa^3\text{-(}S\text{)-mbpam}\}(thf)_n]$ (M = Sc, n = 0, **10**; M = Y, n = 1, **11**; M = Lu, n = 1, **12**). Scandium complexes were isolated as THF-free compounds with a pseudo five-coordinate environment, while yttrium and lutetium complexes were isolated with an octahedral geometry due to the coordination of a THF molecule. The fluxionality of complexes **1**–**12** in solution was investigated by VT NMR spectroscopy. The structures of these compounds were determined by spectroscopic methods and the X-ray crystal structure of **1** was also established. Complexes **1**–**12** are efficient catalysts for the intramolecular hydroamination of aminoalkenes, with TOF values up to 198 h^{-1} obtained at 70 ºC for 2,2-diphenyl-pent-4-enylamine (**13**) on using complex **11** as catalyst. Enantioselectivities of up to 99% ee were achieved in the cyclization of aminoalkene **13** with the single enantiopure complex **12**. The hydroamination reactions show zero-order rate dependence on substrate concentration and first-order rate dependence on catalyst concentration.

Introduction

'These elements (rare-earths) perplex us in our researches, baffle us in our speculations and haunt us in our dreams. They stretch like an unknown sea before us - mocking, mystifying and murmuring strange revelations and possibilities' was the address to the British association in 1887 by Sir William Crookes to highlight the intriguing role that these elements had in the field of chemistry. Since then, inorganic chemists have made room for an ever-growing list of new related compounds of group 3 metals, lanthanides and actinides, and a huge variety of structural arrangements, unique chemical properties, and very specific applications have been reported.[1] Nowadays, the synthesis of new compounds of these elements is one of the most attractive fields for potential applications in homogeneous catalysis, organic synthesis and materials science.[2] Despite this situation, the use of these systems as homogeneous catalysts is largely restricted to the laboratory and there are currently few examples in which they are used on an industrial scale.

Focusing attention on the design of new rare-earth (including the group 3 metals scandium and yttrium) complexes for homogeneous catalysis, the most widely investigated compounds are those bearing Cp-type ligands, not only because they have interesting chemical structures and unique reactivity but also due to their versatile catalytic activity and selectivity in the polymerizations of olefins or conjugated dienes.[3] Recent years have witnessed increased attention on organo-*f*-compounds based on N, O and P heteroatoms for homogenous catalysis. This is due to the fact that the strong metal-ligand bonds can stabilize the high electrophilicity and provide the exceptional and tuneable steric and electronic features required.[4,3d]

Ancillary ligands with multiple coordinating sites and large steric bulk are favoured to stabilize rare-earth metal complexes. In this context, scorpionate compounds with multiple coordination sites have been exploited as ancillary ligands.[5] Amongst them, heteroscorpionates are some of the most versatile tridentate ligands[6] and they are able to coordinate and stabilize a wide variety of *f*-elements. In recent years, different groups have

contributed a great deal to the design of new heteroscorpionate ligands related to the bis(pyrazol-1-yl)methane system with several pendant donor arms, such as carboxylate, dithiocarboxylate, aryloxide, alkoxide, amide, cyclopendienyl, acetamidate, thioacetamidate and amidinate.[7] We recently focused on extending the scope of the chemistry of organo-*f*-elements, plus scandium and yttrium, to the synthesis of heteroscorpionate complexes. The synthetic accessibility, structural arrangements and catalytic performance were studied. Since 2005, when we reported our first work related to scandium and yttrium compounds,[8] our efforts have been focused on the synthesis of new derivatives as potential initiators in the ring-opening polymerization of cyclic esters[9] and in the hydroamination of different aminoalkenes.[10]

In this new contribution to the chemistry of the rare-earth elements, we describe in detail the synthesis and characterization of a new series of achiral and chiral silylamide heteroscorpionate rare-earth compounds. The study of the different structural arrangements in these new entities and their performance in the catalytic hydroamination of aminoalkenes were also explored.

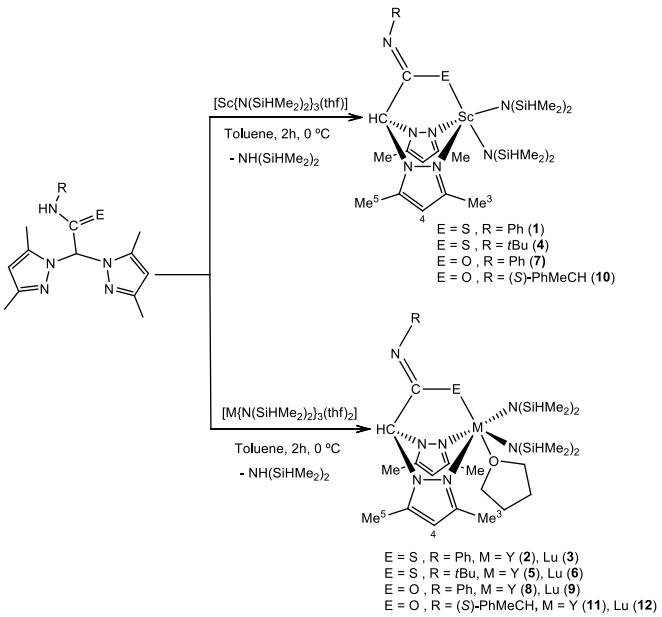

Scheme 1. Synthesis of compounds **1**–**12**.

Results and discussion

Synthesis, structures, and fluxional behaviour. Acetamide or thioacetamide heteroscorpionate precursors contain Lewis basic coordinating groups (N and O or S centres in the 'arm' of the heteroscorpionate moiety) and this makes them an interesting type of ligand for the preparation of rare-earth complexes due to their wide variety of coordination modes.[9,11] Thus, Sc, Y and Lu were the metals chosen to design new complexes that would have interesting features for hydroamination catalysis. The new silylamide compounds [M{N(SiHMe$_2$)$_2$}$_2$(κ^3-pbptam)(thf)$_n$] (M = Sc, **1**, n = 0; M = Y **2**, Lu **3**, n = 1), [M{N(SiHMe$_2$)$_2$}$_2$(κ^3-tbptam)(thf)$_n$] (M = Sc **4**, n = 0; M = Y **5**, Lu **6**, n = 1), [M{N(SiHMe$_2$)$_2$}$_2$(κ^3-pbpam)(thf)$_n$] (M = Sc **7**, n = 0; M = Y **8**, Lu **9**, n = 1) and [M{N(SiHMe$_2$)$_2$}$_2$(κ^3-(*S*)-mbpam}(thf)$_n$] (M = Sc **10**, n = 0; M = Y **11**, Lu **12**, n = 1) were synthesized in a straightforward way by an amine elimination route involving the reaction of the previously reported acetamide and thioacetamide heteroscorpionate protio precursors[9a,b,c] pbptamH [pbptamH = *N*-phenyl-2,2-bis(3,5-dimethylpyrazol-1-yl)thioacetamide], tbptamH [tbptamH = *N*-*tert*-butyl-2,2-bis(3,5-dimethylpyrazol-1-yl)thioacetamide], pbpamH [pbpamH = *N*-phenyl-2,2-bis(3,5-dimethylpyrazol-1-yl)acetamide] and (*S*)-mbpamH [(*S*)-mbpamH = (*S*)-(–)-*N*-α-methylbenzyl-2,2-bis(3,5-dimethylpyrazol-1-yl)acetamide] with 1 *equiv* of the tris(silylamide)complexes [M{N(SiHMe$_2$)$_2$}$_3$(thf)$_n$][12] (n =1, M = Sc; n = 2, M = Y, Lu) (Scheme 1). The reactions were carried out in toluene and, after the appropriate workup, complexes **1**–**6** and **7**–**12** were isolated in *ca.* 80% as yellow and white solids, respectively. The complexes are soluble in THF and toluene but insoluble in *n*-hexane. Scandium complexes were isolated as THF-free compounds. Complexes **10**–**12** were isolated as single enantiopure compounds.

The different acetamidate and thioacetamidate compounds were characterized spectroscopically (see Experimental Section). The ^{13}C NMR signals of the carbonyl and thiocarbonyl groups in these complexes are good indicators of the bonding mode of the acetamidate or thioacetamidate moieties of the ligands. The thiocarbonyl and carbonyl carbon resonances, RN*C*E, are shifted to higher field with respect to those of neutral ligands[9a,b,c,11] (see the Experimental Section), indicating that the acetamidate or thioacetamidate moieties are coordinated to the metal centres through the O or S atoms (see Scheme 1). However, a small amount of delocalized E-C-N double bond probably exists in the acetamidate and thioacetamidate moieties of the heteroscorpionate ligands.

The ^{1}H and ^{13}C{^{1}H} NMR spectra of **1**–**9** (without a chiral carbon) at room temperature show a singlet for each of the H^4, Me^3 and Me^5 pyrazole protons and carbons, indicating that the pyrazoles are equivalent, along with one resonance for the two silylamide ligands and two multiplets for the THF protons in yttrium and lutetium complexes. The ^{1}H and ^{13}C{^{1}H} NMR spectra of **10**–**12** (bearing a stereogenic carbon atom) show two singlets for each of the H^4, Me^3 and Me^5 pyrazole protons and carbons, two signals for the silylamide ligands and two multiplets for the THF protons in yttrium and lutetium complexes (see Fig. 1). These results are consistent with a five coordinate disposition for the scandium complexes and an octahedral structural disposition for the yttrium and lutetium complexes. Thus, these spectroscopic data indicate that the acetamidate or thiacetamidate heteroscorpionate ligands are coordinated in a facial, 'tripodal' fashion with a κ^3-NNE coordination mode. Phase-sensitive ^{1}H NOESY-1D experiments were carried out to confirm the assignment of the signals for the Me^3, Me^5 and H^4 groups of the pyrazole ring and the SiHMe$_2$

group. The assignment of the $^{13}C\{^1H\}$ NMR signals was made on the basis of additional ^1H-^{13}C heteronuclear correlation experiments (g-HSQC).

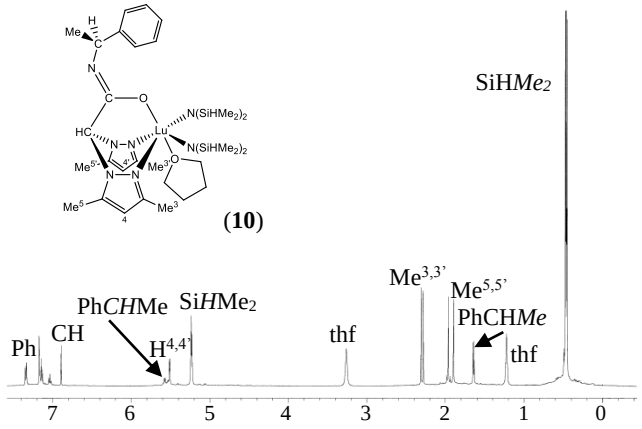

Fig. 1. ^1H NMR spectrum of [Lu{N(SiHMe$_2$)$_2$}$_2${κ^3-(*S*)-mbpam}(thf)] (**10**).

As mentioned above, the scandium compounds have a five-coordinate disposition and in this arrangement, two isomers are possible: one with a square planar pyramidal geometry (Fig. 2a) and another with a trigonal bipyramidal geometry (Fig. 2b). The pyrazole rings are equivalent in both isomers. However, in the first isomer the silylamide ligands are equivalent but in the second they are different, a situation consistent with a square planar pyramidal geometry (Fig. 2a). The room temperature ^1H NMR spectra of the scandium complexes (**1**, **4** and **7**) (with achiral heteroscorpionate ligands) show broad resonances for the two silylamide ligands, indicating the existence of an exchange process between these ligands close to the coalescence temperature. Therefore, the dynamic behaviour of the scandium complexes was studied by VT NMR spectroscopy. In the case of complex **1**, the VT NMR analysis showed that the resonance of the silylamide protons broadens and becomes resolved into a number of separate peaks at low temperature. A stacked plot of the relevant sections of the variable-temperature ^1H NMR spectra of **1** is shown in Fig. 3. At room temperature, the exchange of the silylamide groups occurs and, accordingly, one set of signals is observed. When the temperature was decreased to below 0 ºC, two set of signals were observed for the silylamide ligands (Fig. 3).

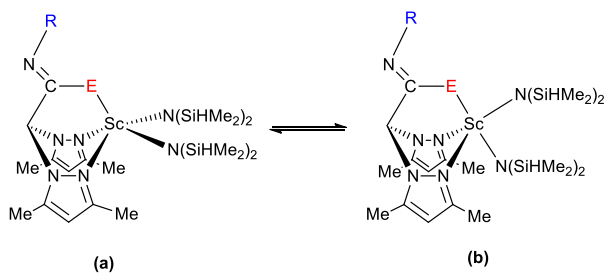

Fig. 2. Proposed structures for the two isomers of scandium complexes.

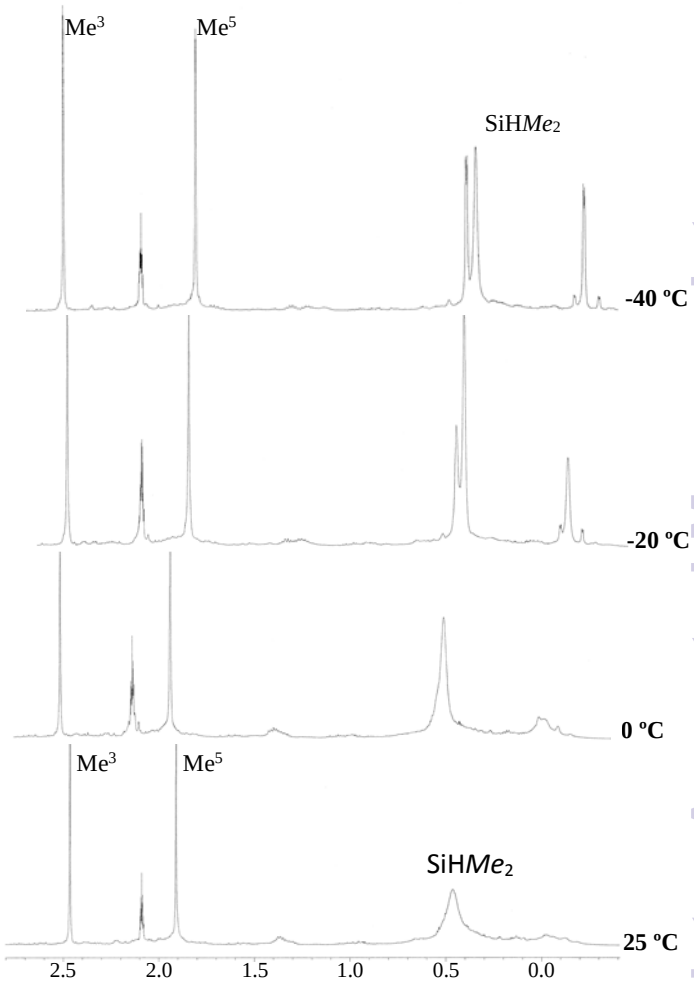

Fig. 3. Variable-temperature ^1H NMR spectra in the region of the methyl groups of compound **1** in toluene-d_8.

A five-coordinate geometry is proposed for Sc compounds, but for derivatives of Y and Lu, which have larger ionic radii, a six-coordinate environment can be considered (Scheme 1). In this arrangement two isomers are possible, *i.e.*, with the *cis* and *trans* disposition of the THF ligand with respect to the oxygen or sulphur atom of the RNCE moiety (Fig. 4). As mentioned previously, the room temperature ^1H NMR spectra of yttrium and lutetium complexes that contain achiral heteroscorpionate ligands show a singlet for each of the H^4, Me^3 and Me^5 pyrazole protons, indicating that the pyrazoles are equivalent. This situation is consistent with the isomer in which the THF ligand is *trans* to the RNCE moiety. However, dynamic behaviour was observed involving the THF group and the silylamide ligands. The VT NMR analysis showed that the resonances of the silylamide and THF ligands directly bonded to the metal centre, as well as those of the pyrazole rings, broaden at –80 ºC and become resolved into a number of separate peaks for each of the ligands present (Fig. S1). Thus, the two pyrazole rings will be not equivalent and this situation is consistent with the isomer in which the THF ligand is *cis* to the RNCE moiety (Fig. 4). It is worth noting that at low temperature, and given the coordination

mode of the ligands, isomers with a *cis* disposition (Fig. 4) are chiral compounds.

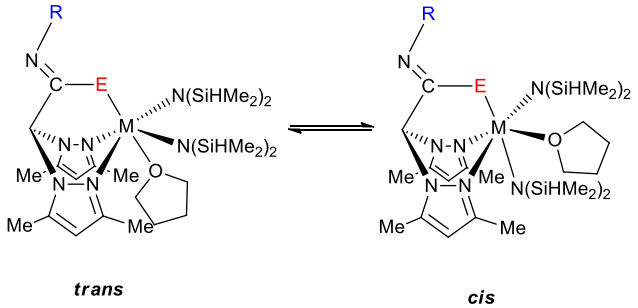

Fig. 4. Proposed structures for the two isomers of yttrium and lutetium complexes.

Conclusive evidence was not found for the presence of *β*-(Si–H) agostic interactions in compounds (**1**–**12**) in solution, a situation that is frequently observed in similar complexes.[13] The ^{1}H NMR spectra show the SiH signals in the range 5.00–5.90 ppm, which is significantly downfield compared to the same SiH resonances from precursor complexes [M{N(SiHMe$_2$)$_2$}$_3$(thf)$_n$].[12] The value of the $^1J_{SiH}$ coupling constant is generally a good tool to gauge the intensity of metal *β*-(Si–H) agostic interactions.[12,13] The $^1J_{SiH}$ values found for complexes **1**–**12** are in the range that is indicative of non-agostic interactions (170–180 Hz) observed in rare-earth complexes.[12,13] Furthermore, it is well known that IR spectroscopy is an efficient method to corroborate the presence of *β*-(Si–H) intramolecular agostic interactions. The Si–H stretching frequencies in the FTIR spectra of **1**–**12** in the solid state are in the region between 1900 and 2200 cm^{-1}, with low-energy shoulders, and this situation indicates the presence of weak agostic *β*-(Si–H) interactions in the solid state.[12,13]

The molecular structure of complex **1** was determined by X-ray diffraction and the ORTEP drawing is depicted in Fig. 5. The crystallographic data and selected interatomic distances and angles are given in Tables 1 and 2, respectively. The molecular structure of **1** determined by X-ray diffraction is in good agreement with the solution structures deduced from the spectroscopic data. The heteroscorpionate ligand is attached to the scandium atom through two nitrogen atoms of pyrazole rings and the sulphur atom from the thioacetamidate moiety in a κ^3-NNS coordination mode with the expected *fac* coordination. In addition, the scandium centre is coordinated to two disilylamide ligands.

A quantitative measure (τ value)[14] has been described to determine the extent of five coordinate geometries. A value of zero identifies a compound as being perfectly square pyramidal and a value of one as perfectly trigonal bipyramidal. The τ value assigned to complex **1** is 0.59 and this confirms a distorted situation between the two five coordination geometries, probably due to the constraints imposed by the heteroscorpionate ligand. This distortion is manifested in the N(1)−Sc(1)−N(3), N(6)−Sc(1)−N(7), N(3)−Sc(1)−N(7) and N(1)−Sc(1)−N(6) angles of 84.8(2)º, 104.5(2)º, 131.4(2)º and 94.2(1)º, respectively.

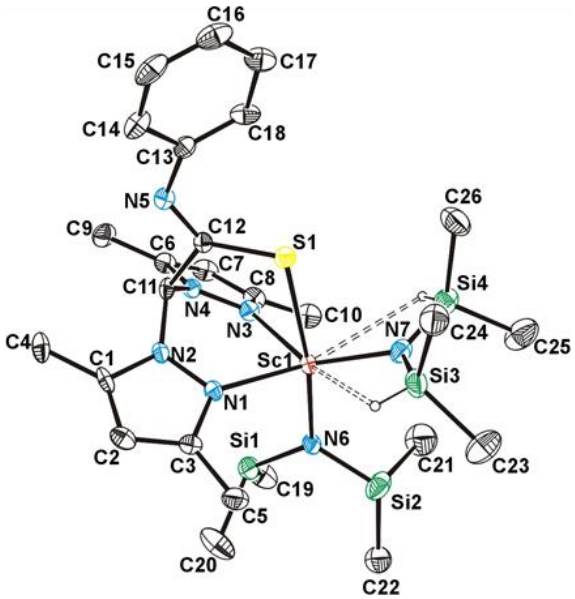

Fig. 5. ORTEP representation of the molecular structure of **1** (ellipsoids drawn at 30% probability). H atoms are omitted for clarity except those that take part in the agostic interactions.

Table 1. Crystal data and structure refinement details for **1**

	1
Molecular formula	$C_{26}H_{48}N_7SScSi_4$
Formula weight	648.09
Temperature (K)	180(2)
Wavelength (Å)	0.71073
Crystal system	Monoclinic
Space group	C 2/c
a (Å)	37.191(5)
b (Å)	10.591(4)
c (Å)	25.678(3)
β (º)	133.52(1)
Volume (Å^3)	7334(3)
Z	8
Density (calculated) (g/cm^3)	1.174
Absorption coefficient (mm^{-1})	0.414
F(000)	2768
Crystal size (mm^3)	0.43 × 0.34 × 0.22
Index ranges	–44 ≤ h ≤ 44 –12 ≤ k ≤ 11 –30 ≤ l ≤ 30
Independent reflections	6244 [R(int) = 0.1955]
Data / restraints / parameters	6244 / 142 / 426
Goodness-of-fit on F^2	0.871
Final R indices [$I>2\sigma(I)$]	R1 = 0.0621 wR2 = 0.1071
Largest diff. peak and hole, e.Å^{-3}	0.277 and –0.245

The distances between the Sc atom and the nitrogen atoms of the pyrazole rings Sc(3)−N(1) and Sc(1)–N(3) [2.264(4) Å and 2.269(4) Å] correlate well with the corresponding distances

found in other scandium pyrazolyl complexes.[9d,e] The bond distances Sc(1)–N(6) of 2.095(4) Å and Sc(1)–N(7) of 2.041(5) Å are similar to the corresponding distances found in other scandium silylamide complexes.[15] These bond lengths are shorter than the Sc–N bond distances from the pyrazole rings, thus confirming that the N atoms of the silylamide ligands are attached to the scandium centre in an anionic fashion. The X-ray diffraction study confirmed the presence of the two *β*-(Si–H) agostic interactions from the same silylamide ligand (symmetric disposition) in the solid state.[13] Thus, the Sc(1)–N(7) bond distance in **1**, 2.041(5) Å, is shorter than those in [Sc{N(SiHMe$_2$)$_2$}$_3$] (average 2.069 Å).[12b] The Sc(1)···Si(3) and Sc(1)···Si(4) contacts of 3.086(3) Å and 3.207(2) Å are comparable with those in the precursor [2.989(1)–3.052(1)][12b] and are shorter than the bond distances Sc(1)–Si(1) and Sc(1)–Si(2) of 3.312(2) Å and 3.321(2) Å, respectively, for the non-interacting silylamide ligand. These symmetric *β*-(Si–H) agostic interactions form two fused four-membered rings, Sc(1)–N(7)–Si(4)–H and Sc(1)–N(7)–Si(3)–H, with a dihedral angle of 4.55º (similar to other symmetric *β*-(Si–H) agostic interactions).[13] Furthermore, relatively acute Sc(1)–N(7)–Si(3) and Sc(1)–N(7)–Si(4) angles of 110.9(3)º and 118.6(3)º are observed. Consequently, the Si(3)–N(7)–Si(4) bond angle, with a value of 129.2(3)º, appears to be slightly widened.

Table 2. Selected bond lengths [Å] and angles [º] for **1**

Bond lengths (Å)		Angles (º)	
Sc(1)–N(1)	2.264(4)	N(6)–Sc(1)–N(7)	104.5(2)
Sc(1)–N(3)	2.269(4)	N(1)–Sc(1)–N(7)	136.1(2)
Sc(1)–N(6)	2.095(4)	N(1)–Sc(1)–N(6)	94.2(1)
Sc(1)–N(7)	2.041(5)	N(3)–Sc(1)–N(7)	131.4(2)
Sc(1)–S(1)	2.648(2)	N(3)–Sc(1)–N(6)	94.6(2)
Sc(1)–Si(3)	3.086(3)	N(1)–Sc(1)–N(3)	84.9(2)
Sc(1)–Si(4)	3.207(2)	N(7)–Sc(1)–S(1)	84.1(1)
Sc(1)–Si(1)	3.312(2)	N(6)–Sc(1)–S(1)	171.4(1)
Sc(1)–Si(2)	3.321(2)	Si(1)–N(6)–Si(2)	118.2(9)
		Si(1)–N(6)–Sc(1)	121.0(2)
		Si(2)–N(6)–Sc(1)	120.3(9)
		Si(4)–N(7)–Si(3)	129.2(3)
		Si(3)–N(7)–Sc(1)	110.9(3)

Hydroamination Catalysis. It is well established that the intramolecular hydroamination/cyclization now constitutes a particularly powerful and concise route to functionalized nitrogen heterocycles.[16] In fact, significant research effort in recent decades has established rare-earth complexes as being highly active catalysts for this process.[16,17]

Complexes **1**–**12** were tested in catalytic intramolecular hydroamination processes. In the initial screening the reactivity was tested in the hydroamination of 2,2-diphenyl-4-pentenylamine (**13**) (Table 3, entries 1–12). The catalytic activity was monitored by ^{1}H NMR spectroscopy in toluene-d$_8$ by loading an NMR tube with catalyst and substrate at room temperature. The results in Table 3 show distinguished catalytic activity for compounds **1**–**12** under mild conditions, with short reaction times and a very low catalyst loading. Unfortunately, the catalytic activities of complexes **1**–**12** in the hydroamination of substrate **13** were lower in comparison to the activity found for the hybrid cyclopentadienyl/scorpionate compounds reported previously.[10] These complexes adhere to the general trend observed for lanthanide-mediated hydroamination, where higher ionic radii correlate with higher catalytic activity. Thus, yttrium complexes showed the highest activity in the hydroamination/cyclization of substrate **13** (see TOF values in Table 3). On the other hand, it is worth noting that complexes **10**–**12**, as single enantiopure compounds, displayed a remarkable asymmetric cyclization of substrate **13** with up to 99% ee achieved (see entries 4, 8 and 12 in Table 3). Yttrium catalyst **11** seems to be the best candidate to examine the scope of complexes **1**–**12** as precatalysts. A variety of aminoalkenes was tested under various reaction conditions. Entries 13–15 (Table 3) correspond to the results obtained, at different [cat]/[substrate], in the hydroamination/cyclization of (1-allylcyclohexyl)methylamine (**14**), which bears a cyclohexyl unit in the geminal position. For this substrate, the catalytic activity is lower than that of **13**, probably due to the significant Thorpe–Ingold effect of the geminal phenyl units in **13**. We also considered the hydroamination/cyclization of an internal 1,2-disubstituted alkene, namely (*E*)-2,2-dimethyl-5-phenyl-4-penten-1-amine (**15**), to give the cyclic product **19** (Table 3, entries 16 and 17). This cyclization reaction required much longer reaction times, higher catalyst loadings and a temperature of 100 ºC to obtain even low yields. We also explored the tandem cyclization reaction of the substrate 2-allyl-2-methylpent-4-enylamine (**16**) with compound **11** (Table 3, entries 18 and 19). The allyl-substituted secondary amine **20** was formed and this did not react further to give the tertiary amine even when the catalytic reaction was carried out under more forcing conditions, namely 100 ºC for four days and with a catalytic loading of 10%. Cyclization of **16** (Table 3, entries 18 and 19) proceeded to give a quantitative yield and two diastereoisomers of pyrrolidine **20** were obtained in similar proportions (Fig. S5, Supporting Information).

Quantitative kinetic studies were carried out on the hydroamination/cyclization of aminoalkene **13** using **11** as the catalyst, with the reaction monitored in situ by ^{1}H NMR spectroscopy (see the Supporting Information). Linear plots of substrate concentration *versus* time were obtained for runs in the range 0.35–0.75 M with the precatalyst concentration kept constant, indicating that the reaction is zero order in substrate concentration (Fig. 6). Furthermore, a linear response was observed for the reaction rate *versus* precatalyt concentration, with the initial substrate concentration kept constant (Fig. 7 and 8), indicating that the reaction is first order in catalyst concentration. This empirical rate law is typical of lanthanide-mediated aminoalkene hydroamination kinetics, which show zero-order dependence on substrate concentration and first-order dependence on precatlyst concentration.[18] The most fruitful comparison is with Marks' lanthanide systems, for which a wealth of mechanistic information is available.[18]

Table 3. Hydroamination/cyclization reaction of aminoalkenes **13-16** catalyzed by complexes **1**–**12**.

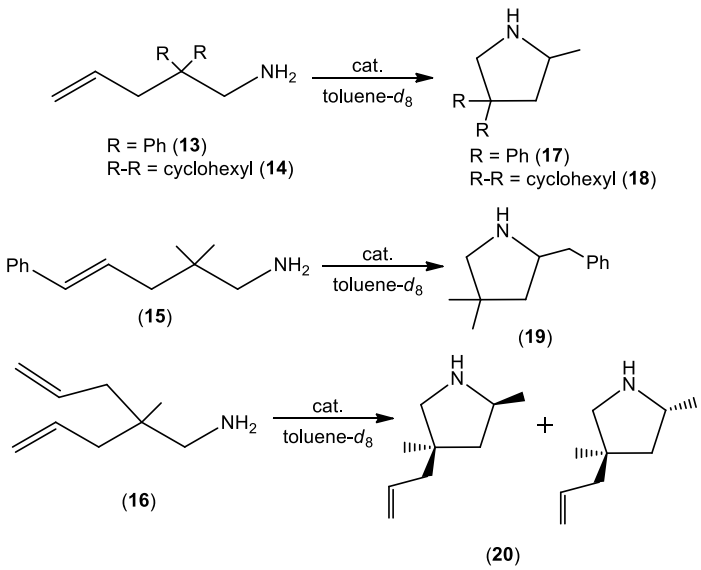

Entry	Subs.	Cat.	t(h)	Yield (%)[b]	TOF (h^{-1})	ee (%)[c]
1	13	1-Sc[a]	0.8	98	122.5	-
2	13	4-Sc[a]	0.9	95	105.5	-
3	13	7-Sc[a]	0.9	92	102.2	-
4	13	10-Sc[a]	0.8	99	123.7	25
5	13	2-Y[a]	0.6	99	165.0	-
6	13	5-Y[a]	0.6	98	163.3	-
7	13	8-Y[a]	0.5	96	192.0	-
8	13	11-Y[a]	0.5	99	198.0	92
9	13	3-Lu[a]	0.7	98	140.0	-
10	13	6-Lu[a]	0.7	94	134.3	-
11	13	9-Lu[a]	0.8	96	120.0	-
12	13	12-Lu[a]	0.7	95	135.7	99
13	14	11-Y[a]	1.0	99	99.0	92
14	14	11-Y[d]	0.6	99	33.0	93
15	14	11-Y[e]	0.2	99	49.5	93
16	15	11-Y[a]	24	traces	-	-
17	15	11-Y[f]	24	48	0.2	-
17	16	11-Y[a]	1.5	99	66.0	-
18	16	11-Y[g]	0.8	99	12.4	-

[a]Toluene-d_8, 70 °C, [cat]/[substrate] = 1%, [b]NMR yield determined relative to ferrocene as internal standard. [c]Enantiomeric excess determined by ^{19}F NMR of Mosher amides. [d]Toluene-d_8, 70 °C, [cat]/[substrate] = 5%. [e]Toluene-d_8, 70 °C, [cat]/[substrate] = 10%. [f]Toluene-d_8, 100 °C, [cat]/[substrate] = 10%. [g]Toluene-d_8, 100 °C, [cat]/[substrate] = 10%.

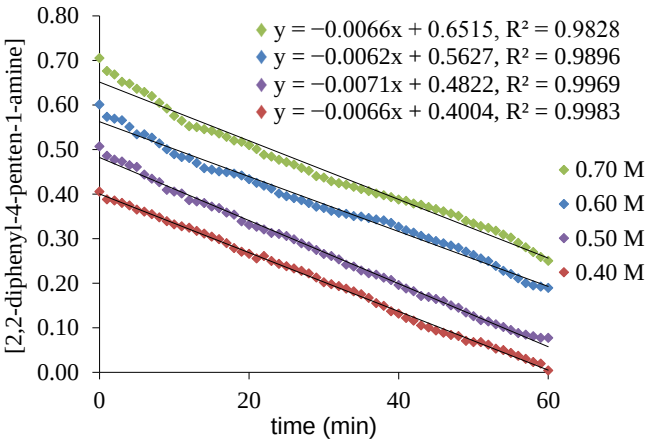

Fig. 6. Linear regression fits for [2,2-diphenyl-4-penten-1-amine] (**13**) *versus* time were obtained for the first 60 min, indicating that the reactions are zero-order in substrate concentration. Plot of [2,2-diphenyl-4-penten-1-amine] *versus* time, illustrating zero-order dependence on [2,2-diphenyl-4-penten-1-amine]. The concentration of catalyst **11** is 0.020 M.

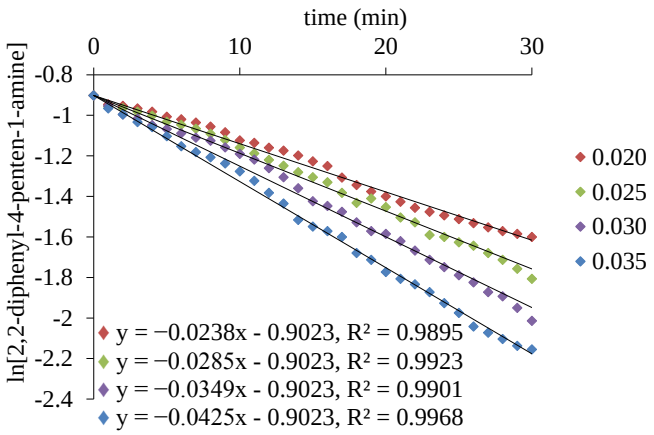

Fig. 7. Linear regression fits for ln[2,2-diphenyl-4-penten-1-amine] (**13**) *versus* time were obtained for the first 30 min. Plot of ln[2,2-diphenyl-4-penten-1-amine] *versus* time for several catalyst (**11**) concentrations (0.020, 0.025, 0.030, 0.035 M). The concentration of substrate [2-diphenyl-4-penten-1-amine] is 0.40 M.

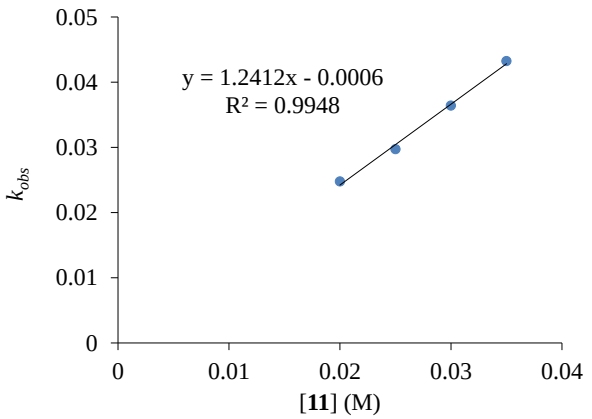

Fig. 8. Plot of k_{obs} (from Fig. 7) *versus* concentration of [Y{N(SiHMe$_2$)$_2$}$_2${κ^3-(*S*)-mbpam}(thf)] (**11**) for the cyclization of 2,2-diphenyl-4-penten-1-amine (**13**) showing first order dependence on catalyst concentration.

Conclusions

The aim of the work described here was to contribute towards the ever-growing library of scandium, yttrium and lutetium compounds and, in particular, of the less common heteroscorpionate organometallic rare-earth metal compounds. Twelve amide heteroscorpionate compounds were prepared and structurally characterized, both in solution and in the solid state. Scandium compounds have a five-coordinate geometry, whereas a molecule of thf is also included with the larger metal centres (Y and Lu) and this gives rise to six-coordinate geometries. The highly fluxional nature of the complexes led us to study the interchange between geometries in both arrangements by VT NMR spectroscopy.

All of the new complexes were tested as catalysts for the hydroamination/cyclization of the aminoalkene 2,2-diphenyl-4-penten-1-amine. The complexes gave good TOF values, under mild conditions, with short reaction times and low catalyst loadings. Amongst them, the yttrium heteroscorpionate single enantiopure compound **11** was chosen to examine the scope of these new entities. Very good values for *ee* are reported for the yttrium and lutetium single enantiopure compounds (**11** and **12**). Finally, three more aminoalkenes were tested in order to expand the substrate scope. Catalyst **11** was successful in the transformation of other aminoalkenes but longer reaction times and a higher catalyst loading were required.

Experimental

General procedure

All manipulations were performed under nitrogen, using standard Schlenk techniques. Solvents were pre-dried over sodium wire (toluene, n-hexane and THF) and distilled under nitrogen from sodium (toluene and THF) or sodium-potassium alloy (*n*-hexane). Deuterated solvents were stored over activated 4 Å molecular sieves and degassed by several freeze-thaw cycles. Microanalyses were carried out with a Perkin-Elmer 2400 CHN analyzer. ^{1}H, ^{13}C, ^{29}Si and ^{19}F NMR spectra were recorded on a Varian Inova FT-500 spectrometer. The NOESY-1D spectra were recorded on a Varian Innova FT-500 with the following acquisition parameters: irradiation time 2 s and number of scans 256, using standard VARIANT-FT software. Two-dimensional NMR spectra were acquired using standard VARIANT-FT software and processed using an IPC-Sun computer. IR spectra were obtained on a Shimadzu IRPrestige-21 spectrophotometer equipped with a Pike Technology ATR system. The specific rotation $[\alpha]_D^{22}$ was measured at 22 ºC on a Perkin-Elmer 241 Polarimeter equipped with a Na lamp operating at 589 nm with a light path length of 10 cm. $ScCl_3$, YCl_3 and $LuCl_3$ were purchased from Aldrich or Strem. Phenyl isocyanate, phenyl isothiocyanate, fluoren-2-yl isocyanate, (S)-(–)-α-methylbenzyl isocyanate and *tert*-butyl isothiocyanate were purchased from Aldrich. The compounds [M{N(SiHMe$_2$)$_2$}$_3$(thf)$_n$],[12] bis(3,5-dimethylpyrazol-1-yl)methane (bdmpzm),[19] bis(3,5-di-*tert*-butylpyrazol-1-yl)methane (bdtbpzm)[19] 2,2-diphenyl-4-penten-1-amine (**13**),[20] (1-allylcyclohexyl)methylamine (**14**),[20] (*E*)-2,2-dimethyl-5-phenyl-4-penten-1-amine (**15**)[20] and 2-allyl-2-methyl-4-penten-1-amine (**16**)[20] were prepared according to literature procedures.

Synthesis of Complexes

[Sc{N(SiHMe$_2$)$_2$}$_2$(κ^3-pbptam)] (1). In a 100 mL Schlenk tube, [Sc{N(SiHMe$_2$)$_2$}$_3$(thf)] (0.40 g, 0.78 mmol) was dissolved in dry toluene (25 mL) and the solution was placed in an ice bath. A solution of the thioacetamide pbptamH (0.26 g, 0.78 mmol) in dry toluene (25 mL) was added. The resulting solution was stirred for 2 h at 0 °C. The solvent was removed under vacuum and the solid was washed with hexane. The resulting solid was crystallized from a mixture of toluene/hexane to give yellow crystals. Yield 90%. Anal. Calcd for $C_{26}H_{48}N_7SScSi_4$: C 48.2, H 7.4, N 15.1. Found: C 48.5, H 7.3, N 15.2. ^{1}H NMR (500 MHz, C_6D_6, 297 K): δ = 7.09 (s, 1H, CH), 7.41 (d, $^3J_{H-H}$ = 7.8 Hz, 2H, *H^o* NPh), 7.15 (t, $^3J_{H-H}$ = 7.2 Hz, 1H, *H^p* NPh), 7.02 (m, 2H, *H^m* NPh), 5.38 (s, 2H, H^4), 5.11 (brs, 4H, SiH), 2.49 (s, 6H, Me^3), 1.87 (s, 6H, Me^5), 0.39 (brs, 24H, SiMe$_2$). ^{13}C{^{1}H} NMR (C_6D_6, 297 K; δ (ppm)): 171.0 (N*C*=S), 150.6, 142.6 (C$^{3 \text{ and } 5}$), 138.8 (*C^{ipso}* NPh), 129.0 (*C^m* NPh), 125.6 (*C^p* NPh), 123.9 (*C^o* NPh), 107.6 (C^4), 76.2 (CH), 15.5 (Me^3), 10.9 (Me^5), 3.8 (SiMe$_2$). ^{29}Si NMR (C_6D_6, 297 K): –22.4 (ds, $^1J_{SiH}$ = 178.1 Hz, $^2J_{SiH}$ = 6.2 Hz, NSiHMe$_2$). IR: ν = 2106 [vs, ν(SiH)], 2044 (m, sh), 1602 (vs), 1556 [s, ν(C=N)] cm^{-1}.

[Y{N(SiHMe$_2$)$_2$}$_2$(κ^3-pbptam)thf] (2). The synthesis procedure was the same as for complex **1**, using [Y{N(SiHMe$_2$)$_2$}$_3$(thf)$_2$] (0.40 g, 0.62 mmol) and pbptamH (0.21 g, 0.63 mmol) to give **2** as a yellow solid. Yield 90%. Anal. Calcd for $C_{30}H_{56}N_7OSSi_4Y$: C 47.2, H 7.4, N 12.8. Found: C 47.8, H 7.7, N 12.3. ^{1}H NMR (500 MHz, C_6D_6, 297 K): δ = 7.03 (s, 1H, CH), 7.40 (d, $^3J_{H-H}$ = 8.0 Hz, 2H, *H^o* NPh), 7.26 (t, $^3J_{H-H}$ = 7.4 Hz, 1H, *H^p* NPh), 6.92 (m, 2H, *H^m* NPh), 5.43 (s, 2H, H^4), 5.29 (brs, 4H, SiH), 3.94 (m, 4H, thf), 2.51 (s, 6H, Me^3), 1.92 (s, 6H, Me^5), 1.31 (m, 4H, thf), 0.40 (brs, 24H, SiMe$_2$). ^{13}C{^{1}H} NMR (125 MHz, C_6D_6, 297 K): δ 172.1 (N*C*=S), 151.1, 142.2 (C$^{3 \text{ and } 5}$), 137.8 (*C^{ipso}* NPh), 129.3 (*C^m* NPh), 123.6 (*C^p* NPh), 122.7 (*C^o* NPh), 107.3 (C^4), 76.1 (CH), 71.2 (thf), 25.2 (thf), 15.6 (Me^3), 11.2 (Me^5), 3.9 (SiMe$_2$). ^{29}Si NMR (C_6D_6, 297 K): –22.5 (ds, $^1J_{SiH}$ = 177.1 Hz, $^2J_{SiH}$ = 8.3 Hz, NSiHMe$_2$). IR: ν = 2020 [vs, ν(SiH)], 1976 (m, sh), 1677 (vs), 1560 [s, ν(C=N)], cm^{-1}.

[Lu{N(SiHMe$_2$)$_2$}$_2$(κ^3-pbptam)thf] (3). The synthesis procedure was the same as for complex **1**, using [Lu{N(SiHMe$_2$)$_2$}$_3$(thf)$_2$] (0.40 g, 0.56 mmol) and pbptamH (0.18 g, 0.56 mmol) to give **3** as a yellow solid. Yield 90%. Anal. Calcd for $C_{30}H_{56}LuN_7OSSi_4$: C 42.4, H 6.6, N 11.5. Found: C 42.3, H 6.6, N 11.4. ^{1}H NMR (500 MHz, C_6D_6, 297 K): δ = 7.23 (s, 1H, CH), 7.20 (d, $^3J_{H-H}$ = 8.0 Hz, 2H, *H^o* NPh), 7.14 (t, $^3J_{H-H}$ = 7.4 Hz, 1H, *H^p* NPh), 6.83 (m, 2H, *H^m* NPh), 5.43 (s, 2H, H^4),

5.29 (brs, 4H, SiH), 3.56 (m, 4H, thf), 1.82 (s, 6H, Me^3), 1.43 (s, 6H, Me^5), 1.37 (m, 4H, thf), 0.47 (brs, 24H, $SiMe_2$). $^{13}C\{^1H\}$ NMR (125 MHz, C_6D_6, 297 K): δ = 184.3 (N*C*=S), 150.2, 140.8 ($C^{3\text{ and }5}$), 138.6 (C^{ipso} NPh), 128.6 (C^m NPh), 125.6 (C^p NPh), 129.3 (C^o NPh), 106.6 (C^4), 64.5 (CH), 69.1 (thf), 25.4 (thf), 13.4 (Me^3), 10.1 (Me^5), 3.8 ($SiMe_2$). ^{29}Si NMR (C_6D_6, 297 K): –22.3 (ds, $^1J_{SiH}$ = 176.2 Hz, $^2J_{SiH}$ = 6.3 Hz, NSi*H*Me_2). IR: ν = 2124 [vs, ν(Si*H*)], 1995 (m, sh), 1630 (vs), 1536 [s, ν(C=N)], cm^{-1}.

[Sc{N(SiHMe_2)$_2$}$_2$(κ^3-tbptam)] (4). The synthesis procedure was the same as for complex **1**, using [Sc{N(SiHMe_2)$_2$}$_3$(thf)] (0.40 g, 0.78 mmol) and tbptamH (0.25 g, 0.78 mmol) to give **4** as a yellow solid. Yield 80%. Anal. Calcd for $C_{24}H_{52}N_7SScSi_4$: C 45.9, H 8.3, N 15.6. Found: C 46.1, H 8.6, N 15.2. ^1H NMR (500 MHz, C_6D_6, 297 K): δ = 6.80 (s, 1H, CH), 5.40 (s, 2H, H^4), 5.40 (brs, 4H, SiH), 2.46 (s, 6H, Me^3), 1.89 (s, 6H, Me^5), 1.50 (s, 9H, ^{t}Bu), 0.40 (brs, 24H, $SiMe_2$). $^{13}C\{^1H\}$ NMR (125 MHz, C_6D_6, 297 K): δ = 178.0 (N*C*=S), 152.7, 144.8 ($C^{3\text{ and }5}$), 107.0 (C^4), 73.5 (CH), 55.4 ($C(CH_3)_3$), 16.7 ($C(CH_3)_3$), 12.9 (Me^3), 10.8 (Me^5), 3.5 ($SiMe_2$). ^{29}Si NMR (C_6D_6, 297 K): –23.4 (ds, $^1J_{SiH}$ = 175.2 Hz, $^2J_{SiH}$ = 6.0 Hz, NSi*H*Me_2). IR: ν = 2048 [vs, ν(Si*H*)], 2114 (m, sh), 1651 (vs), 1545 [s, ν(C=N)], cm^{-1}.

[Y{N(SiHMe_2)$_2$}$_2$(κ^3-tbptam)thf] (5). The synthesis procedure was the same as for complex **1**, using [Y{N(SiHMe_2)$_2$}$_3$(thf)$_2$] (0.40 g, 0.63 mmol) and tbptamH (0.20 g, 0.63 mmol) to give **5** as a yellow solid. Yield 85%. Anal. Calcd for $C_{28}H_{60}N_7OSSi_4Y$: C 45.2, H 8.1, N 13.2. Found: C 45.7, H 8.5, N 13.0. ^1H NMR (500 MHz, C_6D_6, 297 K): δ = 7.03 (s, 1H, CH), 5.49 (s, 2H, H^4), 5.10 (brs, 4H, SiH), 3.95 (m, 4H, thf), 2.48 (s, 6H, Me^3), 1.93 (s, 6H, Me^5), 1.42 (s, 9H, ^{t}Bu), 1.42 (m, 4H, thf), 0.35 (brs, 24H, $SiMe_2$). $^{13}C\{^1H\}$ NMR (125 MHz, C_6D_6, 297 K): δ = 179.5 (N*C*=S), 152.4, 141.5 ($C^{3\text{ and }5}$), 107.2 (C^4), 74.1 (CH), 66.2 (thf), 25.8 (thf), 55.1 ($C(CH_3)_3$), 17.4 ($C(CH_3)_3$), 12.5 (Me^3), 11.6 (Me^5), 3.3 ($SiMe_2$). ^{29}Si NMR (C_6D_6, 297 K): –23.3 (ds, $^1J_{SiH}$ = 177.4 Hz, $^2J_{SiH}$ = 7.3 Hz, NSi*H*Me_2). IR: ν = 2068 [vs, ν(Si*H*)], 1955 (m, sh), 1657 (vs), 1540 [s, ν(C=N)], cm^{-1}.

[Lu{N(SiHMe_2)$_2$}$_2$(κ^3-tbptam)thf] (6). The synthesis procedure was the same as for complex **1**, using [Lu{N(SiHMe_2)$_2$}$_3$(thf)$_2$] (0.40 g, 0.56 mmol) and tbptamH (0.18 g, 0.56 mmol) to give **6** as a yellow solid. Yield 80%. Anal. Calcd for $C_{28}H_{60}LuN_7OSSi_4$: C 40.5, H 7.3, N 11.8. Found: C 40.9, H 7.8, N 11.4. ^1H NMR (500 MHz, C_6D_6, 297 K): δ = 6.75 (s, 1H, CH), 5.25 (s, 2H, H^4), 5.90 (brs, 4H, SiH), 3.76 (m, 4H, thf), 2.30 (s, 6H, Me^3), 1.73 (s, 6H, Me^5), 1.33 (m, 4H, thf), 1.30 (s, 9H, ^{t}Bu), 0.37 (brs, 24H, $SiMe_2$). $^{13}C\{^1H\}$ NMR (125 MHz, C_6D_6, 297 K): δ = 169.0 (N*C*=S), 150.6, 143.0 ($C^{3\text{ and }5}$), 107.4 (C^4), 78.6 (CH), 67.5 (thf), 28.4 (thf), 58.7 ($C(CH_3)_3$), 11.3 ($C(CH_3)_3$), 15.0 (Me^3), 11.9 (Me^5), 3.6 ($SiMe_2$). ^{29}Si NMR (C_6D_6, 297 K): –22.6 (ds, $^1J_{SiH}$ = 175.4 Hz, $^2J_{SiH}$ = 6.2 Hz, NSi*H*Me_2). IR: ν = 2078 [vs, ν(Si*H*)], 1990 (m, sh), 1648 (vs), 1565 [s, ν(C=N)], cm^{-1}.

[Sc{N(SiHMe_2)$_2$}$_2$(κ^3-pbpam)] (7). The synthesis procedure was the same as for complex **1**, using [Sc{N(SiHMe_2)$_2$}$_3$(thf)] (0.40 g, 0.78 mmol) and pbpamH (0.25 g, 0.78 mmol) to give **7** as a white solid. Yield 85%. Anal. Calcd for $C_{26}H_{48}N_7OScSi_4$: C 49.4, H 7.6, N 15.5. Found: C 49.8, H 7.9, N 15.1. ^1H NMR (500 MHz, C_6D_6, 297 K): δ = 6.96 (s, 1H, CH), 7.25 (d, $^3J_{H-H}$ = 7.8 Hz, 2H, H^o NPh), 7.17 (t, $^3J_{H-H}$ = 7.2 Hz, 1H, H^p NPh), 6.87 (m, 2H, H^m NPh), 5.48 (s, 2H, H^4), 5.01 (brs, 4H, SiH), 2.29 (s, 6H, Me^3), 1.74 (s, 6H, Me^5), 0.39 (brs, 24H, $SiMe_2$). $^{13}C\{^1H\}$ NMR (125 MHz, C_6D_6, 297 K): δ = 157.0 (N*C*=O), 150.6, 149.7 ($C^{3\text{ and }5}$), 152.7 (C^{ipso} NPh), 129.3 (C^m NPh), 124.0 (C^p NPh), 122.6 (C^o NPh), 107.7 (C^4), 70.9 (CH), 14.5 (Me^3), 10.9 (Me^5), 2.9 ($SiMe_2$). ^{29}Si NMR (C_6D_6, 297 K): –23.1 (ds, $^1J_{SiH}$ = 170.2 Hz, $^2J_{SiH}$ = 6.0 Hz, NSi*H*Me_2). IR: ν = 2050 [vs, ν(Si*H*)], 2108 (m, sh), 1650 (vs), 1545 [s, ν(C=N)], cm^{-1}.

[Y{N(SiHMe_2)$_2$}$_2$(κ^3-pbpam)thf] (8). The synthesis procedure was the same as for complex **1**, using [Y{N(SiHMe_2)$_2$}$_3$(thf)$_2$] (0.40 g, 0.63 mmol) and pbpamH (0.20 g, 0.63 mmol) to give **8** as a white solid. Yield 85%. Anal. Calcd for $C_{30}H_{56}N_7O_2Si_4Y$: C 48.2, H 7.5, N 13.1. Found: C 48.6, H 7.9, N 12.8. ^1H NMR (500 MHz, C_6D_6, 297 K): δ = 6.72 (s, 1H, CH), 7.55 (d, $^3J_{H-H}$ = 7.8 Hz, 2H, H^o NPh), 7.14 (t, $^3J_{H-H}$ = 7.2 Hz, 1H, H^p NPh), 7.03 (m, 2H, H^m NPh), 5.46 (s, 2H, H^4), 5.12 (brs, 4H, SiH), 3.84 (m, 4H, thf), 2.45 (s, 6H, Me^3), 1.79 (s, 6H, Me^5), 1.35 (m, 4H, thf), 0.36 (brs, 24H, $SiMe_2$). $^{13}C\{^1H\}$ NMR (125 MHz, C_6D_6, 297 K): δ = 158.3 (N*C*=O), 152.8, 147.8 ($C^{3\text{ and }5}$), 151.4 (C^{ipso} NPh), 128.8 (C^m NPh), 124.7 (C^p NPh), 120.3 (C^o NPh), 106.9 (C^4), 71.2 (CH), 67.7 (thf), 25.5 (thf), 13.7 (Me^3), 10.5 (Me^5), 2.8 ($SiMe_2$). ^{29}Si NMR (C_6D_6, 297 K): –24.5 (ds, $^1J_{SiH}$ = 170.3 Hz, $^2J_{SiH}$ = 6.9 Hz, NSi*H*Me_2). IR: ν = 1990 [vs, ν(Si*H*)], 1931 (m, sh), 1675 (vs), 1587 [s, ν(C=N)], cm^{-1}.

[Lu{N(SiHMe_2)$_2$}$_2$(κ^3-pbpam)thf] (9). The synthesis procedure was the same as for complex **1**, using [Lu{N(SiHMe_2)$_2$}$_3$(thf)$_2$] (0.40 g, 0.56 mmol) and pbpamH (0.18 g, 0.56 mmol) to give **9** as a white solid. Yield 85%. Anal. Calcd for $C_{30}H_{56}N_7LuO_2Si_4$: C 43.2, H 6.7, N 11.7. Found: C 43.9, H 7.0, N 11.2. ^1H NMR (500 MHz, C_6D_6, 297 K): δ = 6.97 (s, 1H, CH), 7.24 (d, $^3J_{H-H}$ = 7.5 Hz, 2H, H^o NPh), 7.11 (t, $^3J_{H-H}$ = 7.1 Hz, 1H, H^p NPh), 6.90 (m, 2H, H^m NPh), 5.47 (s, 2H, H^4), 5.15 (brs, 4H, SiH), 3.83 (m, 4H, thf), 2.45 (s, 6H, Me^3), 1.77 (s, 6H, Me^5), 1.36 (m, 4H, thf), 0.37 (brs, 24H, $SiMe_2$). $^{13}C\{^1H\}$ NMR (125 MHz, C_6D_6, 297 K): δ = 157.5 (N*C*=O), 155.5, 141.6 ($C^{3\text{ and }5}$), 152.1 (C^{ipso} NPh), 129.2 (C^m NPh), 125.7 (C^p NPh), 124.9 (C^o NPh), 108.4 (C^4), 71.9 (CH), 66.9 (thf), 27.4 (thf), 14.1 (Me^3), 11.4 (Me^5), 3.1 ($SiMe_2$). ^{29}Si NMR (C_6D_6, 297 K): –24.3 (ds, $^1J_{SiH}$ = 175.8 Hz, $^2J_{SiH}$ = 7.3 Hz, NSi*H*Me_2). IR: ν = 2110 [vs, ν(Si*H*)], 1980 (m, sh), 1659 (vs), 1578 [s, ν(C=N)], cm^{-1}.

[Sc{N(SiHMe_2)$_2$}$_2${κ^3-(*S*)-mbpam}] (10). The synthesis procedure was the same as for complex **1**, using [Sc{N(SiHMe_2)$_2$}$_3$(thf)] (0.40 g, 0.78 mmol) and (*S*)-mbpamH (0.27 g, 0.78 mmol) to give **10** as a white solid. Yield 88%. $[\alpha]_D^{25}$ = –31.3 (*c* 0.10, toluene). Anal. Calcd for $C_{28}H_{52}N_7OScSi_4$: C 51.0, H 8.0, N 14.9. Found: C 51.5, H 8.2, N 14.6. ^1H NMR (500 MHz, C_6D_6, 297 K): δ = 6.96 (s, 1H, CH), 7.37-7.00 (m, 5H, NCH(CH_3)*Ph*), 5.63 (m, 1H, N*CH*(CH_3)Ph), 5.45, 5.42 (s, 2H, $H^{4,4'}$), 5.35 (brs, 4H, SiH), 1.90, 2.28 (s, 3H each, $Me^{3,3'}$), 1.83, 2.25 (s, 3H each, $Me^{5,5'}$), 1.60 (d, $^3J_{H-H}$ = 6.5 Hz, 3H, NCH(*CH*$_3$)Ph), 0.39 (brs, 24H, $SiMe_2$). $^{13}C\{^1H\}$ NMR (125 MHz, C_6D_6, 297 K): δ = 161.5 (N*C*=O), 148.9, 148.7, 141.5, 141.2 ($C^{3,3'\text{ or }5,5'}$), 146.9 (C^{ipso} NCH(CH_3)*Ph*), 128.3 (C^m NCH(CH_3)*Ph*), 126.9 (C^p NCH(CH_3)*Ph*), 127.4 (C^o NCH(CH_3)*Ph*), 106.3, 106.0 ($C^{4,4'}$), 69.5 (CH), 51.4 (N*C*H(CH_3)Ph), 24.9 (NCH(*C*H$_3$)Ph), 13.6, 13.5 ($Me^{3,3'}$), 11.4, 11.3 ($Me^{5,5'}$), 3.4 ($SiMe_2$). ^{29}Si NMR (C_6D_6, 297 K): –24.8 (ds, $^1J_{SiH}$ = 173.5 Hz, $^2J_{SiH}$ = 6.7 Hz, NSi*H*Me_2). IR: ν = 2015 [vs, ν(Si*H*)], 1989 (m, sh), 1612 (vs), 1592 [s, ν(C=N)], cm^{-1}.

[Y{N(SiHMe_2)$_2$}$_2${κ^3-(*S*)-mbpam}thf] (11). The synthesis procedure was the same as for complex **1**, using [Y{N(SiHMe_2)$_2$}$_3$(thf)$_2$] (0.40 g, 0.63 mmol) and (*S*)-mbpamH (0.22 g, 0.63 mmol) to give **11** as a white solid. Yield 85%. $[\alpha]_D^{25}$

= –24.6 (*c* 0.10, toluene). Anal. Calcd for $C_{32}H_{60}N_7O_2Si_4Y$: C 49.5, H 7.8, N 12.6. Found: C 49.9, H 8.1, N 12.0. ^{1}H NMR (500 MHz, C_6D_6, 297 K): δ = 6.87 (s, 1H, CH), 7.35-7.00 (m, 5H, NCH(CH$_3$)*Ph*), 5.57 (m, 1H, N*CH*(CH$_3$)Ph), 5.50, 5.48 (s, 2H, H$^{4,4'}$), 5.30 (brs, 4H, SiH), 3.30 (m, 4H, thf), 1.97, 2.31 (s, 3H each, Me$^{3,3'}$), 1.95, 2.28 (s, 3H each, Me$^{5,5'}$), 1.62 (d, $^3J_{H-H}$ = 6.6 Hz, 3H, NCH(*CH$_3$*)Ph), 1.22 (m, 4H, thf), 0.39 (brs, 24H, SiMe$_2$). ^{13}C{^{1}H} NMR (125 MHz, C_6D_6, 297 K): δ = 162.2 (N*C*=O), 148.7, 148.6, 141.1, 141.0 (C$^{3,3'\text{ or }5,5'}$), 146.8 (*C^{ipso}* NCH(CH$_3$)*Ph*), 128.8 (*C^m* NCH(CH$_3$)*Ph*), 126.7 (*C^p* NCH(CH$_3$)*Ph*), 127.3 (*C^o* NCH(CH$_3$)*Ph*), 106.2, 106.0 (C$^{4,4'}$), 69.6 (CH), 68.4 (thf), 25.2 (thf), 51.3 (N*C*H(CH$_3$)Ph), 22.3 (NCH(*C*H$_3$)Ph), 13.3, 13.0 (Me$^{3,3'}$), 11.2, 11.1 (Me$^{5,5'}$), 3.3 (SiMe$_2$). ^{29}Si NMR (C_6D_6, 297 K): –25.1 (ds, $^1J_{SiH}$ = 177.3 Hz, $^2J_{SiH}$ = 6.0 Hz, NSiHMe$_2$). IR: ν = 2101 [vs, ν(SiH)], 1963 (m, sh), 1632 (vs), 1540 [s, ν(C=N)], cm^{-1}.

[Lu{N(SiHMe$_2$)$_2$}$_2${κ^3-(*S*)-mbpam}thf] (12). The synthesis procedure was the same as for complex **1**, using [Lu{N(SiHMe$_2$)$_2$}$_3$(thf)$_2$] (0.40 g, 0.56 mmol) and (*S*)-mbpamH (0.20 g, 0.56 mmol) to give **12** as a white solid. Yield 84%. $[\alpha]_D^{25}$ = –36.1 (*c* 0.10, toluene). Anal. Calcd for $C_{32}H_{60}LuN_7O_2Si_4$: C 44.6, H 7.0, N 11.4. Found: C 44.8, H 7.5, N 11.0. ^{1}H NMR (500 MHz, C_6D_6, 297 K): δ = 6.89 (s, 1H, CH), 7.40-7.00 (m, 5H, NCH(CH$_3$)*Ph*), 5.65 (m, 1H, N*CH*(CH$_3$)Ph), 5.56, 5.54 (s, 2H, H$^{4,4'}$), 5.25 (brs, 4H, SiH), 3.25 (m, 4H, thf), 1.95, 2.31 (s, 3H each, Me$^{3,3'}$), 1.88, 2.28 (s, 3H each, Me$^{5,5'}$), 1.65 (d, $^3J_{H-H}$ = 6.6 Hz, 3H, NCH(*CH$_3$*)Ph), 1.20 (m, 4H, thf), 0.56 (d, $^3J_{H-H}$ = 3.2 Hz, 12H, SiMe$_2$), 0.50 (d, $^3J_{H-H}$ = 3.1 Hz, 12H, SiMe$_2$). ^{13}C{^{1}H} NMR (125 MHz, C_6D_6, 297 K): δ = 162.0 (N*C*=O), 148.9, 148.8, 141.3, 141.0 (C$^{3,3'\text{ or }5,5'}$), 146.8 (*C^{ipso}* NCH(CH$_3$)*Ph*), 128.3 (*C^m* NCH(CH$_3$)*Ph*), 126.8 (*C^p* NCH(CH$_3$)*Ph*), 127.8 (*C^o* NCH(CH$_3$)*Ph*), 106.4, 106.1 (C$^{4,4'}$), 69.7 (CH), 68.5 (thf), 22.5 (thf), 51.4 (N*C*H(CH$_3$)Ph), 22.5 (NCH(*C*H$_3$)Ph), 13.4, 13.3 (Me$^{3,3'}$), 11.3, 11.2 (Me$^{5,5'}$), 3.5 (SiMe$_2$). ^{29}Si NMR (C_6D_6, 297 K): –23.8 (ds, $^1J_{SiH}$ = 172.1 Hz, $^2J_{SiH}$ = 6.4 Hz, NSiHMe$_2$). IR: ν = 1998 [vs, ν(SiH)], 1976 (m, sh), 1682 (vs), 1535 [s, ν(C=N)], cm^{-1}.

General procedure for catalytic intramolecular hydroamination

In a typical small scale experiment, 0.01 mmol (0.0065 g) of catalyst [Sc{N(SiHMe$_2$)$_2$}$_2$(κ^3-pbptam)] (**1**) and 1.00 mmol (0.2377 g) of aminoalkene 2,2-diphenyl-4-penten-1-amine (**13**)[20] were dissolved in toluene-d$_8$ (0.75 mL) and placed in a J. Young-style NMR tube with a re-sealable Teflon valve. The tube was closed and placed into an oil bath that was preheated at the desired temperature. The reaction was monitored at regular intervals by ^{1}H NMR spectroscopy to determine the optimum conversion.

X-ray crystallographic structure determination

A summary of crystal data collection and refinement parameters is given in Table 1. Single crystals of **1** were mounted on a glass fibre and transferred to a Bruker X8 APEX II CCD-based diffractometer equipped with a graphite monochromated Mo-Kα radiation source (λ = 0.71073 Å). For this compound, only crystals of low quality (*R*int = 0.196) could be grown and the crystal diffracted poorly. Data were integrated using SAINT[21] and an absorption correction was performed with the program SADABS.[22] The software package SHELXTL version 6.10[23] was used for space group determination, structure solution and refinement by full-matrix least-squares methods based on F^2. The one SiMe$_3$ group showed disorder, which was modelled on three positions by using the DELU and SIMU instructions. All non-hydrogen atoms were refined with anisotropic thermal parameters. Except the hydrogen atoms of Si atoms, the hydrogen atoms were included in the structure factor calculation at idealized positions and were allowed to ride on the neighbouring atoms with relative isotropic displacement coefficients. The hydrogen atoms of Si atoms have included in an idealized position with a distance Si-H of 1.4 Å and then fixed.

Acknowledgements

We gratefully acknowledge financial support from the Ministerio de Economia y Competitividad (MINECO), Spain (Grant No. CTQ2011-22578 and CTQ2014-51912-REDC) and the Junta de Comunidades de Castilla-La Mancha, Spain (Grant No. PEII-2014-013-A).

Notes and references

[a,b,c]Universidad de Castilla-La Mancha, Departamento de Química Inorgánica, Orgánica y Bioquímica-Centro de Innovación en Química Avanzada (ORFEO-CINQA). [a]Facultad de Ciencias y Tecnologías Químicas. 13071-Ciudad Real, Spain. [b]Facultad de Farmacia. 02071-Albacete, Spain. [c]Escuela Técnica Superior de Ingenieros Industriales, 13071 Ciudad Real, Spain.

Electronic Supplementary Information (ESI) available: Experimental details, procedures for catalytic intramolecular hydroamination; kinetic measurements and representative kinetic plots. CCDC reference number 1059154.

1 (a) The Rare Earth Elements: Fundamentals and Application. D. A. Atwood. 2013, John Wiley & Sons, Ltd.; (b) Lanthanide and Actinide Chemistry. S. Cotton. 2006, John Wiley & Sons, Ltd.

2 See as examples: (a) G. Zhang, Y. Wei, L. Guo, X. Zhu, S. Wang, S. Zhou and X. Mu, *Chem.–Eur. J.*, 2015, **21**, 2519; (b) F. T. Edelmann, *Coord. Chem. Rev.*, 2014, **26**, 173; (c) F. T. Edelmann, *Chem. Soc. Rev.*, 2012, **41**, 7657; (d) J. Gromada, J. F. Carpentier and A. Mortreux, *Coord. Chem. Rev.*, 2004, **248**, 397; (e) S. Hong and T. J. Marks, *Acc. Chem. Res.*, 2004, **37**, 673; (f) Z. M. Hou and Y. Wakatsuki, *Coord. Chem. Rev.*, 2002, **231**, 1; (g) S. Arndt and J. Okuda, *Chem. Rev.* 2002, **102**, 1953; (h) G. A. Molander and J. A. C. Romero, *Chem. Rev.*, 2002, **102**, 2161.

3 See as examples: (a) J.-F. Liu, F.-X. Pan, S. Yao, X. Min, D. Cui and Z.-M. Sun, *Organometallics*, 2014, **33**, 1374; (b) P.-H. Wei, L. Xu, L.-C. Song, W.-X. Zhang and Z. Xi, *Organometallics*, 2014, **33**, 2784; (c) Y. Luo, S. Chi and J. Chen, *New J. Chem.* 2013, **37**, 2675; (d) M. Zimmermann and R. Anwander, *Chem. Rev.*, 2010, **110**, 6194; (e) K. C. Jantunen, B. L. Scott, J. C. Gordon and J. L. Kiplinger, *Organometallics*, 2007, **26**, 2777; (f) L. Zhang, Y. Luo and Z. Hou, *J. Am. Chem. Soc.*, 2005, **127**, 14562.

4 See as examples: (a) B. Liu, L. Li, G. Sun, J. Liu, M. Wang, S. Li and D. Cui, *Macromolecules*, 2014, **47**, 4971; (b) M. Hasegawa, H. Ohtsu, D. Kodama, T. Kasai, S. Sakurai, A. Ishiia and K. Suzukic, *New J. Chem.*, 2014, **38**, 1225; (c) H.-M. Ye, N. Ren, J.-J. Zhang, S.-J. Sun and J.-F. Wang, *New J. Chem.*, 2010, **34**, 533; (d) W. E. Piers and D. J. H. Emslie, *Coord. Chem. Rev.*, 2002, **131**, 233.

5 (a) N. Marques, A. Sella and J. Takats, *Chem. Rev.*, 2002, **102**, 2137; (b) F. T. Edelmann, *Angew. Chem., Int. Ed. Engl.*, 2001, **40**, 1656; (c) I. Santos and N. Marques, *New J. Chem.*, 1995, **19**, 551.

6 (a) I. Márquez-Segovia, A. Lara-Sánchez, A. Otero, J. Fernández-Baeza, J. A. Castro-Osma, L. F. Sánchez-Barba and A. M. Rodríguez, *Dalton Trans.*, 2014, **43**, 9586; (b) A. Otero, J. Fernández-Baeza, A. Lara-Sánchez and L. F. Sánchez-Barba, *Coord. Chem. Rev.*, 2013, **257**, 1806.

7 See as examples: (a) M. Honrado, A. Otero, J. Fernández-Baeza, L. F. Sánchez-Barba, A. Garcés, A. Lara-Sánchez and A. M. Rodríguez, *Organometallics*, 2014, **33**, 1859; (b) M. Honrado, A. Otero, J. Fernández-Baeza, L. F. Sánchez-Barba, A. Lara-Sánchez, J. Tejeda, M. P. Carrión, J. Martínez-Ferrer and A. Garcés, A. M. Rodríguez, *Organometallics*, 2013, **32**, 3437; (c) Z. Zhang and D. Cui, *Chem.–Eur. J.* 2011, **17**, 11520; (d) A. Otero, J. Fernández-Baeza, J. Tejeda, A. Lara-Sanchez, S. Franco, J. Martínez-Ferrer, M. P. Carrión, I. López-Solera, A. M. Rodríguez and L. F. Sánchez-Barba, *Inorg. Chem.*, 2011, **50**, 1826; (e) G. Türkoglu, C. P. Ulldemolins, R. Müller, E. Hübener, F. W. Heinemann, M. Wolf and N. Burzlaff, *Eur. J. Inorg. Chem.*, 2010, 2962; (f) A. Otero, J. Fernández-Baeza, J. Tejeda, A. Lara-Sanchez, M. Sánchez-Molina, S. Franco, M. I. López-Solera, A. M. Rodríguez, L. Sánchez-Barba, S. Morante-Zarcero and A. Garcés, *Inorg. Chem.*, 2009, **48**, 5540; (g) R-Y. Tan, J. Hong, M. Du and L-F. Tang, *J. Organomet. Chem.*, 2007, **692**, 1708; (h) R. G. Howe, C. S. Tredget, S. C. Lawrence, S. Subongkoj, A. R. Cowley and P. Mountford, *Chem. Commun.*, 2006, 223.

8 A. Otero, J. Fernández-Baeza, A. Antiñolo, J. Tejeda, A. Lara-Sánchez, L. Sánchez-Barba, E. Martínez-Caballero, A. M. Rodríguez and I. López-Solera, *Inorg. Chem.*, 2005, **44**, 5336.

9 (a) A. Otero, A. Lara-Sánchez, J. Fernández-Baeza, C. Alonso-Moreno, I. Márquez-Segovia, L. F. Sánchez-Barba, J. A. Castro-Osma and A. M. Rodríguez, *Dalton Trans.*, 2011, **40**, 4687; (b) A. Otero, A. Lara-Sánchez, J. Fernández-Baeza, E. Martínez-Caballero, I. Márquez-Segovia, C. Alonso-Moreno, L. F. Sánchez-Barba, A. M. Rodríguez and I. López-Solera, *Dalton Trans.*, 2010, **39**, 930; (c) A. Otero, J. Fernández-Baeza, A. Lara-Sánchez, C. Alonso-Moreno, I. Márquez-Segovia, L. F. Sánchez-Barba and A. M. Rodríguez, *Angew. Chem.*, 2009, **48**, 2176; (d) A. Otero, J. Fernández-Baeza, A. Lara-Sánchez, A. Antiñolo, J. Tejeda, E. Martínez-Caballero, I. Márquez-Segovia, I. López-Solera, L. F. Sánchez-Barba and C. Alonso-Moreno, *Inorg. Chem.*, 2008, **47**, 4996; (e) A. Otero, J. Fernández-Baeza, A. Antiñolo, A. Lara-Sánchez, E. Martínez-Caballero, J. Tejeda, L. F., Sánchez-Barba, C. Alonso-Moreno and I. López-Solera, *Organometallics*, 2008, **27**, 976; (f) A. Lara-Sánchez, A. Rodríguez, D. L. Hughes, M. Schormann and M. Bochmann, *J. Organomet. Chem.*, 2002, **663**, 63.

10 A. Otero, A. Lara-Sánchez, C. Nájera, J. Fernández-Baeza, I. Márquez-Segovia, J. A. Castro-Osma, J. Martínez, L. F. Sánchez-Barba and A. M. Rodríguez, *Organometallics*, 2012, **31**, 2244.

11 (a) A. Otero, A. Lara-Sánchez, J. Fernández-Baeza, C. Alonso-Moreno, J. A. Castro-Osma, I. Márquez-Segovia, L. F. Sánchez-Barba, A. M. Rodríguez and J. C. García-Martínez, *Organometallics*, 2011, **30**, 1507; (b) A. Otero, A. Lara-Sánchez, J. Fernández-Baeza, C. Alonso-Moreno, J. Tejeda, J. A. Castro-Osma, I. Márquez-Segovia, L. F. Sánchez-Barba, A. M. Rodríguez and M. V. Gómez, *Chem.–Eur. J.*, 2010, **16**, 8615.

12 (a) S. Arndt, T. P. Spaniol and J. Okuda, *Chem. Commun.*, 2002, 896. (b) R. Anwander, O. Runte, J. Eppinger, G. Gerstberger, E. Herdtweck and M. Spiegler, *J. Chem. Soc., Dalton Trans.*, 1998, 847. (c) J. L. Atwood, W. E. Hunter, R. D. Rogers, J. Holton, J. McMeeking, R. Pearce and M. F. Lappert, *J. Chem. Soc., Chem. Commun.*, 1978, 140. (d) M. F. Lappert and R. J. Pearce, *Chem. Soc., Chem. Commun.*, 1973, 126.

13 (a) H. J. Yuen and T. J. Marks, *Organometallics*, 2008, **27**, 155. (b) W. Hieringer, J. Eppinger, R. Anwander and W. A. Herrmann, *J. Am. Chem. Soc.*, 2000, **122**, 11983. (c) L. J. Procopio, P. J. Carroll and D. H. Berry, *J. Am. Chem. Soc.*, 1994, **116**, 177.

14 (a) M.–A. Muñoz-Hernandez, T. S. Keizer, P. Wei, S. Parkin and D. A. Atwood, *Inorg. Chem.*, 2001, **40**, 6782; (b) J. Muller and R. Boese, *J. Mol. Struct.*, 2000, **520**, 215.

15 (a) H. Ma, T. P. Spaniol and J. Okuda, *Angew. Chem., Int. Ed.*, 2006, **45**, 7818; (b) C. S. Tredgdet, S. C. Lawrence, B. D. Ward, G. R. Howe, A. R. Cowley and P. Mountford, *Organometallics*, 2005, **24**, 3136; (c) H. Ma, T. P. Spaniol and J. Okuda, *Dalton Trans.*, 2003, 4770; (d) F. Estler, E. Herdtwck and R. Anwander, *J. Chem. Soc., Dalton Trans.*, 2002, 3088; (e) P. B. Hitchcock, M. F. Lappert and A. Singh, *J. Chem. Soc., Chem. Commun.*, 1983, 1499.

16 (a) T. E. Müller, K. C. Hultzsch, M. Yus, F. Foubelo and M. Tada, *Chem. Rev.*, 2008, **108**, 3795; (b) F. Pohlki and S. Doye, *Chem. Soc. Rev.*, 2003, **32**, 104; (c) J. J. Brunet and D. Neibecker, *In Catalytic Heterofunctionalization*, A. Togni, and H. Gruetzmacher, Eds.; Wiley-VCH: Weinheim, Germany, 2001; pp 91−141.

17 See as examples: (a) K. Manna, A. Ellern and A. D. Sadow, *Chem. Commun.*, 2010, **46**, 33.; (b) D. C. Leitch, P. R. Payne, C. R. Dunbar and L. L. Schafer, *J. Am. Chem. Soc.*, 2009, **131**, 18246. (d) B. D. Stubber and T. J. Marks, *J. Am. Chem. Soc.*, 2007, **129**, 6149; (e) D. V. Gribkov and K. C. Hultzsch, *Angew. Chem., Int. Ed.*, 2004, **43**, 5542; (f) J.-S. Li, Y. Ryu and T. J. Marks, *J. Am. Chem. Soc.*, 2003, **125**, 12584.

18 See as examples: (a) M. R. Gagné, C. L. Stern and T. J. Marks, *J. Am. Chem. Soc.*, 1992, **114**, 275; (b) M. R. Gagné and T. J. Marks, *J. Am. Chem. Soc.*, **1989**, *111*, 4108–4109.

19 (a) A. Beck, B. Weibert and N. Burzlaff, *Eur. J. Inorg. Chem.*, 2001, 521; (b) E. Díez-Barra, A. de la Hoz, A. Sánchez-Migallon and J. Tejeda, *J. Chem. Soc., Perkin Trans.*, 1993, **1**, 1079; (c) J. Sebastian, P. Sala, J. Del Mazo, M. Sancho, C. Ochia, J. Elguero, J. P. Fayet and M. C. Vertut, *Heterocycl. Chem.*, 1982, **19**, 1141.

20 P. Hornillo-Martinez, K. C. Hultzsch, F. Hampel, *Chem. Commun.*, 2006, 2221.

21 SAINT+ v7.12a. Area-Detector Integration Program. Bruker-Nonius AXS. Madison, Wisconsin, USA, 2004.

22 G. M. Sheldrick, SADABS version 2004/1. A Program for Empirical Absorption Correction. University of Göttingen, Göttingen, Germany, 2004.
23 SHELXTL-NT version 6.12. Structure Determination Package. Bruker-Nonius AXS. Madison, Wisconsin, USA, 2001.

Table of Contents for

Synthesis and Structural Characterization of Amido Heteroscorpionate Rare-Earth Metals Complexes. Hydroamination of Aminoalkenes

Antonio Otero,[a,*] Agustín Lara-Sánchez,[a,*] Jose A. Castro-Osma,[a] Isabel Márquez-Segovia,[a] Carlos Alonso-Moreno,[b] Juan Fernández-Baeza,[a] Luis F. Sánchez-Barba,[a] Ana M. Rodríguez[c].

New amide heteroscorpionate rare-earth complexes were developed and used as efficient catalysts for the intramolecular hydroamination of aminoalkenes